Cold Regions Science and Technology 76-77 (2012) 24–36

Contents lists available at ScienceDirect

Cold Regions Science and Technology

journal homepage: www.elsevier.com/locate/coldregions

Advances in understanding ice–ocean stress during and since AIDJEX

Miles G. McPhee *

McPhee Research Company, 450 Clover Springs Road, Naches, WA 98937, USA

ARTICLE INFO

Article history:
Received 9 February 2011
Received in revised form 26 April 2011
Accepted 3 May 2011

Keywords:
Ice/ocean drag
Turbulent stress
Rossby similarity
Underice hydraulic roughness

ABSTRACT

Variation of ice/ocean drag (momentum exchange) is an important yet often overlooked aspect of pack ice modeling. It is commonly parameterized as proportional to the square of the velocity difference between the ice and the undisturbed ocean, often with a constant angle offset to account for rotational effects in the ice–ocean boundary layer. This approach is critiqued in light of extensive observations that have revealed the underlying turbulence scales governing momentum exchange within the IOBL. Fluid dynamical similarity implied by these scales provides a framework for addressing several factors that affect the drag relationship, including variation in ice roughness, relative drift speed, buoyancy flux at the ice/ocean interface, and stratification in the upper ocean. These are examined and discussed in light of recent changes in the Arctic ice pack. The drag law is formulated in terms of dimensionless surface velocity, which in its simplest form is called Rossby similarity, and accounts explicitly for variation in undersurface hydraulic roughness, z_0. A generalization that includes interfacial buoyancy flux is also described and illustrated, and the impact of near surface ocean stratification is discussed. Estimates of z_0 based on underice measurements vary widely; by a combination of observations and simple IOBL modeling, an attempt is made to reduce these to a manageable set associated with distinct ice types.

1. Introduction

In 1974, the final year of my thesis project under Prof. J. D. Smith in the Geophysics Program at the University of Washington, I was recruited by Max Coon to join the AIDJEX (Arctic Ice Dynamics Joint Experiment) Modeling Group, with primary responsibility for addressing the "ocean stress" term in the force balance for Arctic pack ice. Thus began a long collaboration and friendship with Max that gave me great personal satisfaction, and incidentally, did much to nurture my career as a scientist. As time progressed, I came to realize that beneath that jovial exterior (which almost always put people around him at ease), Max was an exceptionally gifted organizer, who was tenacious in getting what had to be done, done. He led the AIDJEX Modeling Group, and had assembled a talented collection of scientists from diverse backgrounds, many of whom have remained friends over what has become several decades since we all worked together in a building left from a defunct auto dealership on Roosevelt Avenue in Seattle.

As opposed to earlier, thermodynamics-only ice models (e.g., Maykut and Untersteiner, 1971), the thrust of the AIDJEX modeling effort was to understand and predict the dynamics of sea ice, which meant properly describing its momentum balance. For most practical purposes, the balance comprises (*i*) the local time rate of change of momentum; (*ii*) the Coriolis force in a rotating (fixed to earth) reference frame; (*iii*) the net force from internal stress gradients within the ice column; and (*iv*) and (*v*) the traction vectors exerted by the atmosphere and ocean, respectively. Since sea ice was often observed to respond directly to wind changes, it was recognized early on (e.g., Ekman, 1905) that the last two terms would often be important; hence appreciable observational effort was exerted during AIDJEX to understand wind and water stress. Since I had done my graduate work with Prof. Smith analyzing upper ocean stress measurements from the 1972 AIDJEX Pilot Study, Max apparently felt that I could contribute by applying the field results to the modeling effort. It was a wonderful opportunity for me.

Stress at the ice/water interface is a manifestation of turbulent exchange within a relatively thin layer (typically around 20–50 m thick) in the upper ocean: the ice–ocean boundary layer (IOBL). In the introduction to his seminal paper, Ekman (1905) described how Nansen had observed that the *Fram*, during its famous drift, "followed the wind's direction, but deviated 20–40° the right, … a consequence of the earth's rotation." Ekman went on to mathematically describe the effect of rotation on the structure of the planetary boundary layers, deriving the elegant spiral in velocity, now bearing his name, that is fundamental to understanding geophysical fluid dynamics. A fascinating feature of the IOBL is that it is one of the few places where the Ekman spiral can be observed directly. Despite strong inferential evidence of Ekman turning, it was more than half a century after Ekman's prediction that the first unequivocal example of a boundary-layer spiral in nature was published by Hunkins (1966), using a

* Tel./fax: +1 509 658 2575.
E-mail addresses: mmcphee@hughes.net, miles@mcpheeresearch.com.

0165-232X/$ – see front matter © 2011 Elsevier B.V. All rights reserved.
doi:10.1016/j.coldregions.2011.05.001

composite of current profiles measured from sea ice over a two-month period at Arctic Drift Station Alpha during IGY in 1958. Hunkins assumed that stress remained nearly constant in a shear layer between the ice/water interface and the level at which the angle between stress and current was 45°, which he identified as the upper limit of the Ekman layer, with velocity $\hat{v}_E$.[1] By fitting his measurements to an Ekman spiral, Hunkins derived a value for eddy viscosity in the ocean: $0.0024\ m^2\ s^{-1}$. Under the assumption that eddy viscosity is truly constant, the Ekman solution provides a linear relationship between kinematic stress and near surface velocity. A linear drag coefficient with constant turning thus more or less represented the state of the art at the onset of the AIDJEX program in the early 1970s.

In this work, my objective is to trace the evolution of our understanding of momentum exchange at the ice/water interface beginning from AIDJEX. In it, I put particularly strong emphasis on *similarity* in rotating, planetary boundary layers, of which the IOBL constitutes a small subset. There is, of course, an extensive literature on the complex and challenging theory and modeling of turbulent oceanic and atmospheric boundary layers, and no attempt is made here to summarize that work. Rather, I hope to show that relatively simple similarity concepts, in which we seek by appropriate scaling, to reduce a whole class of fluid regimes to a single equation, can explain much about how the ocean exerts drag on the ice underside.

To someone interested only in the drag exerted by the ocean on drifting sea ice (my primary responsibility in Max's modeling group), an extended discussion of similarity may seem esoteric, perhaps beside the point. In my experience, most ice/ocean models express drag using one scalar drag coefficient and a constant turning angle: common values are similar to those used by Hibler (1979) taken from the high range of values I reported for the 1975–76 AIDJEX main experiment (McPhee, 1980); namely, $c_w = 0.0055$; $\beta = 23^o$. There are several reasons why it is important to delve deeper into the drag issue. First, a constant drag coefficient neglects the fact that observed differences in undersurface hydraulic roughness have large impact on both c_w and β. This is particularly important in the Arctic, where phenomenal changes in the ratio of first- to multiyear ice have occurred in recent years (Nghiem et al., 2007), and there is evidence of increased ice mobility and average drift speed due to reduction in ice pack strength and, perhaps, changes in atmospheric circulation. Second, a perennial problem with interpreting underice stress measurements is that from strictly practical considerations, we tend to deploy instrumentation under relatively undeformed ice, perhaps biasing our estimates of the actual exchanges. This was a major issue during the planning for the SHEBA (Surface Heat Budget of the Arctic) project in the late 1990s — the "scaling-up" problem. A third factor is the impact of stratification, also gaining increased prominence because of large changes in freshwater distribution in the Arctic (McPhee et al. 2009). The similarity approach, which evolved from Smith's pioneering turbulence measurements during the 1972 AIDJEX Pilot Study, and which I was able to pursue during my tenure at AIDJEX, provides a rational method for addressing these issues.

The paper is organized as follows. Section 2 describes ice–ocean stress, and its dependence on rotation (Coriolis force) as first illuminated with remarkable clarity in Ekman's (1905) paper. Section 3 introduces the basic concepts of IOBL similarity, melding surface-layer meteorological concepts with outer (Ekman) layer dynamics in a framework called Rossby similarity. Section 4 discusses the impact of buoyancy, incorporating an extension of Rossby similarity approach to include the impact of ice melting. Underside hydraulic roughness, which varies widely for sea ice, is the subject of Section 5, and the paper is summarized in Section 6, along with some recommendations for incorporating the similarity concepts in numerical models.

2. Ice–ocean stress

It is customary to express the stress on the ice underside in terms of the vector velocity difference between the ice and the undisturbed ocean velocity at the far extent of the IOBL (i.e., "far-field" velocity), denoted here in complex notation by $\hat{v}_0$. For drifting sea ice, the actual surface velocity is the vector sum of $\hat{v}_0$ and geostrophic surface current (possibly modified by tidal currents).

Expressing stress as a linear function of $\hat{v}_0$ is attractive from a computational standpoint, but lacks justification on physical grounds. First, Ekman's original work did not stipulate *constant* eddy viscosity, but rather that it was depth invariant over much of the IOBL. Indeed, with amazing insight based partly on the setup of sea level along the Norwegian coast during storms, Ekman postulated that in the open ocean the turbulent exchange coefficient now called eddy viscosity would vary with wind speed squared (i.e., with the kinematic surface stress). As shown below, this implies that the drag coefficient based on $\hat{v}_E$ would be quadratic instead of linear (more consistent with atmospheric formulations for near surface wind). Second, it was also known that the change in velocity across the so-called constant stress layer between the interface and the upper limit of the Ekman layer would depend in some way on surface roughness. Intuitively, we suspect that for two floes with a force balance that produces the same ocean stress, hence Ekman velocity, if the underside of one floe is smoother than the other, the smooth floe will drift faster.

By analogy with turbulent drag from wind near the surface, kinematic stress (stress divided by density) is often expressed as a quadratic function of $\hat{v}_0$, with a rotation angle, β,

$$\hat{\tau}_0 = c_w v_0 \hat{v}_0 e^{\pm i\beta}. \tag{1}$$

The sign of β in the complex exponential depends on the hemisphere (+ northern), and its function is to rotate the direction of the stress traction vector relative to the surface velocity. Eq. (1), with constant parameters c_w and β, is the most common form of the stress/velocity relation used in ice models. However, in atmospheric boundary layer studies, it is often noted that the relationship between surface stress and the geostrophic wind (proportional to the gradient of the pressure field) is *not* quadratic. With a simple transformation, equations governing the atmospheric and oceanic boundary layer are analogous, leading us to examine the underpinnings of Eq. (1) in light of turbulence measurements in the IOBL.

As part of 1972 AIDJEX Pilot Study, Smith directed an experiment that addressed the primary issues of ice/ocean momentum exchange (Smith, 1972). Smith's apparatus provided the first comprehensive measurement of mean currents and turbulence covariance quantities at several levels through an entire rotational boundary layer, using small ducted current meters arranged in triads so as to measure three-dimensional currents (Smith, 1974), fixed to mast sections suspended from the ice. I was involved in the 1972 fieldwork, and based my dissertation on its results, some of which are useful for illustrating the issues mentioned above. Consider mean velocity measurements made during a windstorm we experienced during the Pilot Study (Fig. 1). Velocities are shown relative to a level determined by other means to be near the vertical extent of the turbulent IOBL.[2] A 5-h period of rapid and relatively steady ice drift occurred on the afternoon (local time) of Apr 12, followed on Apr 13 by a relatively steady 8-h period of drift in the almost the same direction, but with diminished speed (McPhee and Smith, 1976). Despite distortions from a true Ekman spiral in the

[1] Herein horizontal vectors are expressed as complex numbers: e.g., $\hat{v}_E = v_{Ex} + iv_{Ey}$ where v_{Ex} and v_{Ey} are components in a horizontal, orthogonal reference frame. Quantities written without carets denote scalar magnitude.

[2] For conditions on Apr 13 (Fig. 1B), the dynamic boundary layer depth was approximately 12 m less than the pycnocline depth, which had been set by stronger vertical mixing on the previous day.

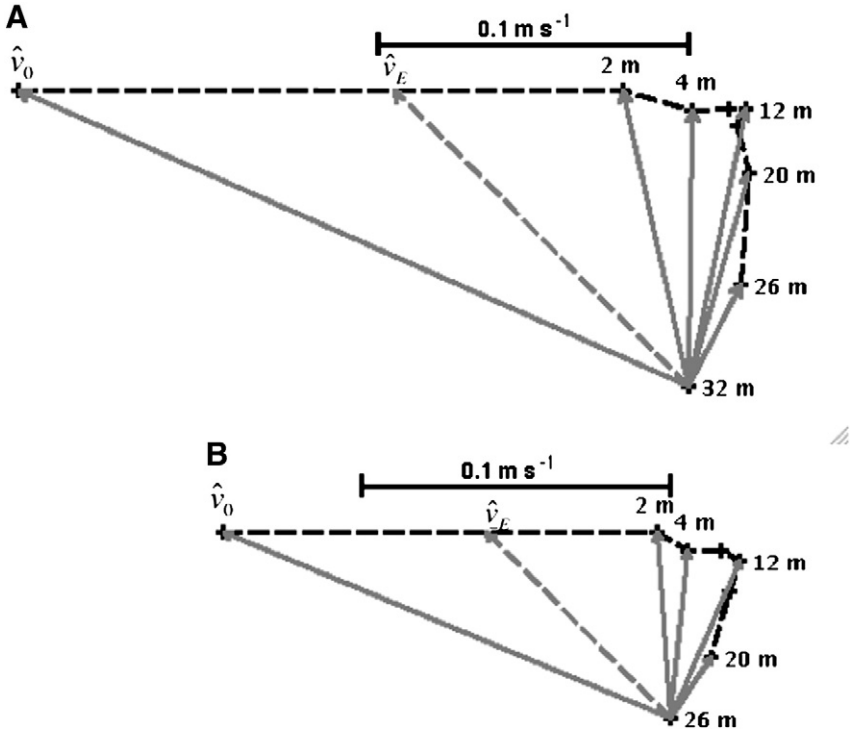

Fig. 1. Plan view (hodograph) of currents measured at depths shown (from the ice undersurface) relative to geostrophic flow averaged over a 5-h period on 12 Apr 1972 at the AIDJEX Pilot Study site (A) and averaged for 8 h on 13 Apr (B), drawn to the same scale. To illustrate the spiraling structure, vectors are drawn relative to the current measured at levels of minimum turbulent kinetic energy, where absolute velocity was small. The dashed vector drawn between the ice and 2 m level corresponds to $\hat{v}_E$, the Ekman surface velocity.

two profiles, probably associated with inhomogeneities in the underice surface, it is clear that rotation played a major role in the velocity structure. Assuming the interfacial stress to be in the same direction as the current shear between the 2-m level and the ice interface, $\hat{v}_E$ lies between the interface and 2 m, hence the assumption of constant stress is probably not unreasonable.

3. IOBL similarity

Possibly the most important result from the Pilot Study IOBL turbulence studies, which might appear obvious in retrospect but was little recognized at the time, is that the IOBL is dynamically similar to the atmospheric boundary layer. We demonstrated this (McPhee and Smith, 1976) by showing reasonable correspondence between direct estimates of the Reynolds stress tensor and eddy viscosity in the upper ocean, and results of numerical atmospheric boundary layer models that had only recently appeared in the literature, as shown, e.g., in Fig. 2. Note that in the figure, the actual diagonal components of the Reynolds stress tensor ($\langle u'u' \rangle$, etc.) are divided by the surface kinematic stress magnitude (u_{*0}^2), where vector friction velocity is defined by $\hat{\tau}_0 = u_{*0}\hat{u}_{*0}$, i.e., a velocity scale in the direction of kinematic stress with the square root of its magnitude. Similarly, vertical displacement is multiplied by f/u_{*0}, where f is the Coriolis parameter, twice the vertical component of the earth's angular

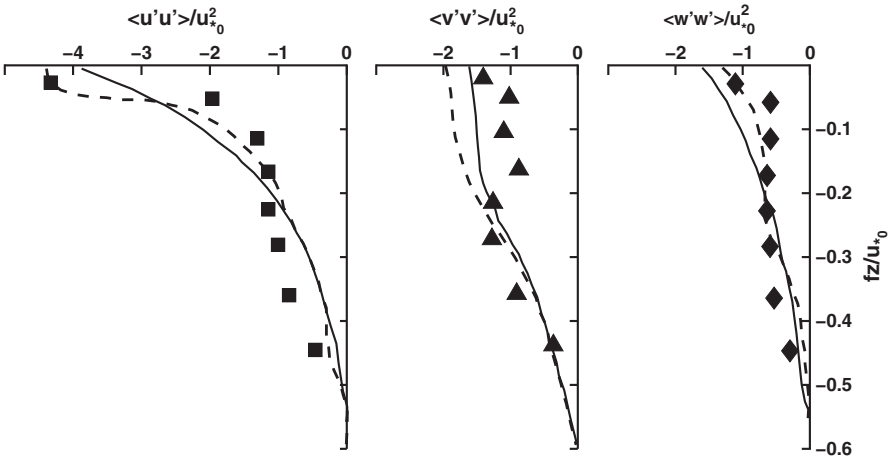

Fig. 2. Dimensionless profiles of the diagonal elements of the Reynolds stress tensor from early planetary boundary layer models (Wyngaard et al., 1974: solid; Deardorff, 1972: dashed) compared with measured values averaged for 5 h during a storm at the AIDJEX Pilot Study site.
From McPhee and Smith (1976).

rotation rate. The similarity implied by the friction velocity scale, $\hat{u}_{*0}$, and the planetary length scale, u_{*0}/f, is critical to understanding the momentum transfer between the ice cover and the ocean, and occupied much of my research as a member of Max's AIDJEX modeling group, particularly in analyzing results from the 1975–76 main AIDJEX experiment, where we lacked direct IOBL turbulence measurements.

The reasoning underlying dynamic similarity may be illustrated as follows. Our goal is to relate the ocean stress to $\hat{v}_0$, the velocity change across the boundary layer. The steady, horizontally homogeneous equation of motion in the IOBL is

$$if\hat{u} = \frac{\partial \hat{\tau}}{\partial z}. \tag{2}$$

Define dimensionless stress ($\hat{\mathrm{T}}$), velocity ($\hat{U}$), and vertical coordinate (ζ) such that $\hat{\tau} = u_{*0}\hat{u}_{*0}\hat{\mathrm{T}}$, $\hat{u} = \hat{u}_{*0}\hat{U}$, and $z = \varsigma u_{*0}/f$. Substituting these into Eq. (2),

$$i\hat{U} = \frac{\partial \hat{T}}{\partial \zeta}. \tag{3}$$

Ekman's insight was to relate stress to the vertical derivative of velocity by analogy with molecular viscosity: $\hat{\tau} = K_m \partial \hat{u} / \partial z$. Ekman assumed that in most of the IOBL the proportionality factor, K_m, was independent of z. Substituting the dimensionless variables defined above, we obtain

$$\hat{T} = \frac{fK_m}{u_{*0}}\frac{\partial \hat{U}}{\partial \zeta} = K_* \frac{\partial \hat{U}}{\partial \zeta} \tag{4}$$

where K_* is dimensionless eddy viscosity. So far, this is just mathematical manipulation; however, the *similarity hypothesis* is that if the scales have been chosen properly, one dimensionless equation describes the whole class of flows under consideration: in our case, steady, horizontally homogeneous, neutrally buoyant (i.e., negligible density gradient) boundary layers. If this holds, then K_* must be constant for the whole class, hence dimensional eddy viscosity is proportional to interfacial stress: $K_m = K_* u_{*0}^2/f$. As noted above, Ekman (1905) suggested that eddy viscosity would vary as the square of the wind speed, which in turn is proportional to surface stress in the open ocean.

Eqs. (3) and (4) may be combined to obtain a second-order partial differential equation in either $\hat{U}$ or $\hat{\mathrm{T}}$. For example,

$$\frac{\partial^2 \hat{T}}{\partial \zeta^2} - \frac{i}{K_*}\hat{\mathrm{T}} = 0 \tag{5}$$

subject to boundary conditions $\hat{\mathrm{T}}(\zeta \to -\infty) = 0$ and $\hat{\mathrm{T}}(\zeta = 0) = \frac{\hat{\tau}_0}{u_{*0}\hat{u}_{*0}} = 1$, with solution

$$\hat{\mathrm{T}} = e^{\hat{\boldsymbol{\delta}}\zeta}$$
$$\hat{\boldsymbol{\delta}} = \sqrt{i/K_*} = \frac{1+i}{\sqrt{2K_*}}. \tag{6}$$

The complex combination $\hat{\boldsymbol{\delta}}\zeta$ both rotates and attenuates stress with increasing depth ($-\zeta$), hence produces a spiral in stress as well as velocity. We observed a stress profile (Fig. 3) in the IOBL during the 1992 Ice Station Weddell project in the western Weddell Sea (McPhee and Martinson, 1994) suggestive of an ideal Ekman stress profile. The vectors represent our estimate of turbulent stress from the covariance of horizontal velocity with vertical velocity, i.e., $\hat{\tau} = u'w' + iv'w'$, where primes denote deviatory currents (mean removed) while the dashed curve is the Ekman stress spiral according to Eq. (6), with the surface stress chosen to make the solution match the measured stress at 4 m. In the southern hemisphere, f is negative, so stress rotates counterclockwise with increasing depth. Note that there has been

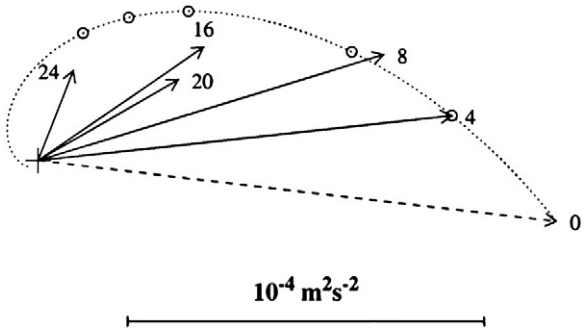

Fig. 3. Turbulent stress measured at 5 levels during a storm at Ice Station Weddell in 1992. The dotted curve is an idealized Ekman stress spiral with $K_* = 0.02$. Adapted from McPhee and Martinson (1994).

significant rotation and attenuation of the horizontal stress traction vector within the first 4 m of the water column.

Since the AIDJEX Pilot Study, several projects from sea ice in both hemispheres have verified the choice of similarity scales (for an extensive summary, see McPhee, 2008a, Ch. 5). Given the premise that a simple Ekman spiral with depth invariant eddy viscosity can approximate the turbulent stress distribution in the IOBL, then it follows that the relationship between interfacial stress magnitude and Ekman speed (v_E) is quadratic. If stress is considered constant in the thin surface layer above the Ekman (outer) layer, and the vertical origin is set at the bottom of the surface layer, it is easily verified that the dimensionless Ekman velocity is

$$\hat{U}_E = \frac{\hat{v}_E}{\hat{u}_{*0}} = \frac{1}{\sqrt{2K_*}}(1-i) \tag{7}$$

which implies that $v_E \propto u_{*0}$, or equivalently, $\tau_0 \propto v_E^2$. While a number of assumptions are involved in arriving at the quadratic stress/velocity relationship for the outer layer, this result appears to be quite robust.

If the ice velocity actually did correspond to $\hat{v}_E$, similarity would dictate a "universal" drag coefficient

$$c_{DE} = K_* e^{i\pi/4} \tag{8}$$

where the complex exponential rotates the stress vector 45° from the Ekman velocity. As Fig. 1 illustrates, $\hat{v}_0$ is considerably larger than the inferred Ekman velocity and the angle between $\hat{v}_0$ and interfacial stress is more like half the canonical 45°.[3] Obviously we need to consider what happens in the shear layer between the ice and the upper limit of the Ekman layer.

From a combination of measurements from AIDJEX and several polar projects since, along with theory and modeling, four length scales emerge as controlling the turbulent exchange process in the IOBL (McPhee, 2008a, Ch. 5): (*i*) the planetary scale, u_{*0}/f, as already discussed; (*ii*) the distance from the boundary; (*iii*) the Obukhov length, which introduces buoyancy into the problem as discussed below; and (*iv*) the vertical extent of the well mixed layer between the surface and pycnocline. Generally, the smallest of these scales governs turbulent exchange at any level. For neutrally buoyant IOBLs (little melting or freezing, deep pycnocline), (*iii*) and (*iv*) are too large to be pertinent. Either by analogy with molecular viscosity, or simply by dimensional arguments, eddy viscosity is the product of a length

[3] That multiyear pack ice is often observed to deflect about 45° from the surface wind is as much a function of the Coriolis force acting on the ice mass as it is Ekman turning in the IOBL.

scale (λ) and a velocity scale (u_τ). Near the boundary of a neutrally buoyant shear flow, it is well established that the velocity profile is very close to logarithmic (the *law of the wall*), and that current shear is well described by the dimensionless shear expression:

$$\phi_m = \frac{\kappa|z|}{\hat{u}_{*0}}\frac{\partial \hat{u}}{\partial z} = 1 \tag{9}$$

where $\kappa = 0.4$ is Kármán's constant. Since kinematic stress is $u_{*0}\hat{u}_{*0} = K_m \partial \hat{u} / \partial z$, it immediately follows from Eq. (9) that obvious choices for the eddy viscosity scales in the surface layer are $u_\tau = u_{*0}$ and $\lambda = \kappa|z|$. I have found that a workable definition of surface layer is the region near the boundary where the mixing length, λ, varies linearly with distance from the interface. Under the assumption that stress remains almost constant through the surface layer, the similarity eddy viscosity K_* provides an estimate of the surface layer extent. Let $K_{max} = K_* u_{*0}^2/f$ be the depth invariant eddy viscosity in the outer (Ekman) layer. It follows that $\lambda_{max} = K_* u_{*0}/f$ in the outer layer, which matches the linear increase in the surface layer when $|z_{sl}| = \lambda_{max}/\kappa$. Thus the actual surface layer extent is a dynamic variable, but one that remains constant in the similarity sense

$$|\zeta_{sl}| = f|z_{sl}| / u_{*0} = K_* / \kappa. \tag{10}$$

Note that the maximum "dimensionless mixing length" is $\Lambda_* = \kappa f|z_{sl}|/u_{*0} = K_*$, and may be used interchangeably with the maximum dimensionless eddy viscosity. By considering several different factors including gradient in Reynolds stress near the ice/ocean boundary (discussed below), we determined (McPhee and Smith, 1976) that friction speed corresponding to the velocity hodograph depicted in Fig. 1A was about $u_{*0} = 0.01$ m s^{-1}. This is enough information to estimate a representative value of the hydraulic roughness of the ice underside, z_0, for the particular Pilot Study conditions on Apr 12 (Fig. 4A). The "law of the wall" integral of Eq. (9) across the entire surface layer is

$$\frac{\kappa \Delta \hat{u}}{\hat{u}_{*0}} = \log|z_{sl}| + C = \log\frac{|z_{sl}|}{z_0} = \log\frac{K_*}{\kappa} + \log\frac{u_{*0}}{f z_0} \tag{11}$$

where $C = -\log z_0$ is the integration constant, and we have assumed that $\Delta\hat{u}$ is in the same direction as the constant stress traction vector in the surface layer. Given $\Delta\hat{u} = \mathrm{Re}\{\hat{v}_0 - \hat{v}_E\}$, the corresponding value of z_0 is about 30 mm, quite typical of multiyear pack ice. If instead we prescribe $z_0 = 1$ mm, typical of first year ice in the Weddell Sea (McPhee et al., 1999), surface velocity is significantly greater, and the turning angle about 7° less (Fig. 4B).

In this idealization of a pure Ekman spiral, capped by a constant-stress surface layer obeying the law of the wall, ice velocity is $\hat{v}_0 = \hat{v}_E + \Delta\hat{u}$, hence a combination of Eqs. (7) and (11) constitutes a drag relationship:

$$\frac{\hat{v}_0}{\hat{u}_{*0}} = \frac{1}{\kappa}\left[\log\frac{u_{*0}}{f z_0} + \log\frac{K_*}{\kappa} + \frac{1}{\sqrt{2K_*}}(1 \mp i)\right] \tag{12}$$

where the sign of the imaginary component depends on the hemisphere (- north). The right-hand side of Eq. (12) comprises all constants except for the logarithm of the ratio of the planetary scale to the hydraulic roughness, and is simplified to

$$\hat{\Gamma} = \frac{\hat{v}_0}{\hat{u}_{*0}} = \frac{1}{\kappa}[\log Ro_* - A \mp iB] \tag{13}$$

where $Ro_* = u_{*0}/(f z_0)$ is the *surface friction Rossby number*. The expression (Eq. 13) is called Rossby similarity after pioneering work on atmospheric geostrophic drag by C.-G. Rossby in the 1930s (Rossby, 1932; but see also Blackadar and Tennekes, 1968, who first

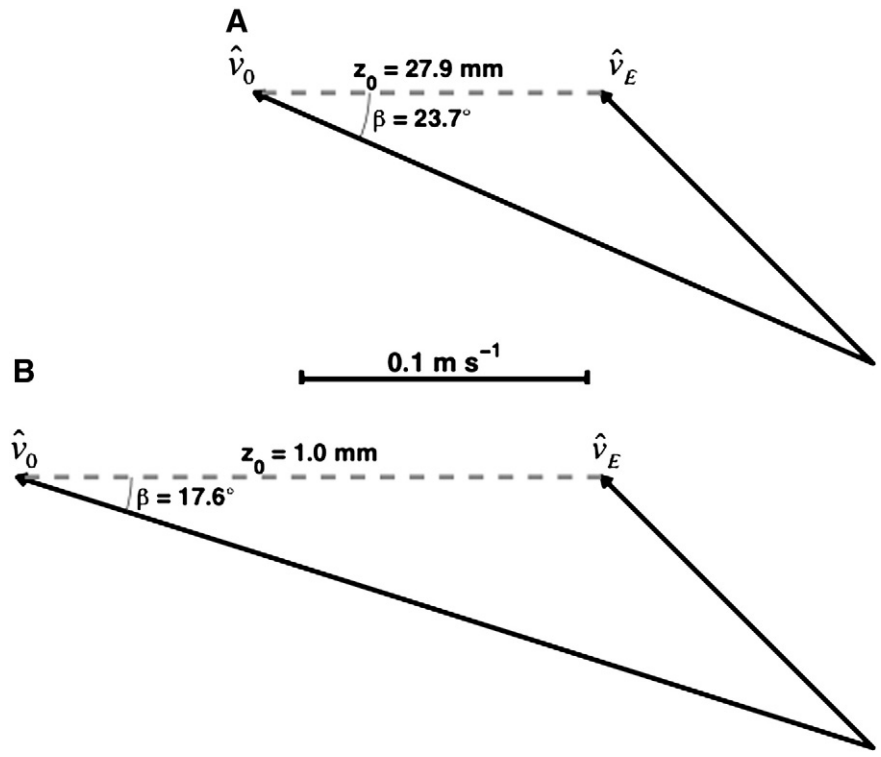

Fig. 4. Impact of different undersurface hydraulic roughness on surface velocity for the same surface stress and Ekman velocities. β is the IOBL turning angle between $\hat{\tau}_0$ and $\hat{v}_0$. *A* corresponds to the AIDJEX current hodograph from Fig. 1A; *B* is with z_0 typical of first year ice.

expressed Ro_* in terms of u_{*_0} instead of free stream velocity). In Eq. (13), the parameters A and B may be treated either as empirical values to be determined from statistics of stress and velocity measurements, or calculated from basic principles as in Eq. (12). For the latter, it is important to note that our definition of *surface layer* is based on the assumption of linearly increasing mixing length ($\lambda = \kappa|z|$), rather than constant stress, and that we expect small but significant attenuation and turning of the stress vector between the interface and z_{sl}. This effect can be approximated by Taylor's series expansion of the exponential dimensionless stress (McPhee, 2008a, Ch. 4), and adds additional terms that modify slightly the analytic expressions implied by Eq. (12):

$$A = -\log\frac{\Lambda_*}{\kappa} - \frac{\kappa}{\sqrt{2\Lambda_*}} + 1 + \sqrt{\frac{\Lambda_*}{2\kappa^2}}$$
$$B = -\frac{\kappa}{\sqrt{2\Lambda_*}} + \sqrt{\frac{\Lambda_*}{2\kappa^2}}. \quad (14)$$

In Eq. (14), K_* has been replaced by Λ_*, its equivalent in the simple model set forth so far. As one might expect, however, relaxing the requirement that stress remain constant in the surface layer also increases Λ_* because of diminished stress at the top of the outer layer. Based on extensive measurements in the outer layer (e.g., McPhee, 1994), combined with more sophisticated IOBL modeling, a representative value is $\Lambda_* \approx 0.028$, which provides analytic values: $A = 2.3$, $B = 2.0$. These values agree reasonably well with various empirical estimates: $A = 1.9$, $B = 2.1$ from AIDJEX (McPhee 1979); $A = 2.1$ $B = 2.3$ from SHEBA (McPhee, 2008a, Ch. 9); $A = 2.4$, $B = 2.3$ from unmanned Arctic Ocean instrumented buoys (Shaw et al., 2008).

The dimensionless surface velocity relative to the undisturbed ocean, $\hat{\Gamma}$, is the inverse of a geostrophic drag relation. Note that Eq. (13) is implicit in u_{*0}, so to the degree that the ice/ocean system obeys Rossby similarity, the stress/velocity relationship cannot be quadratic.

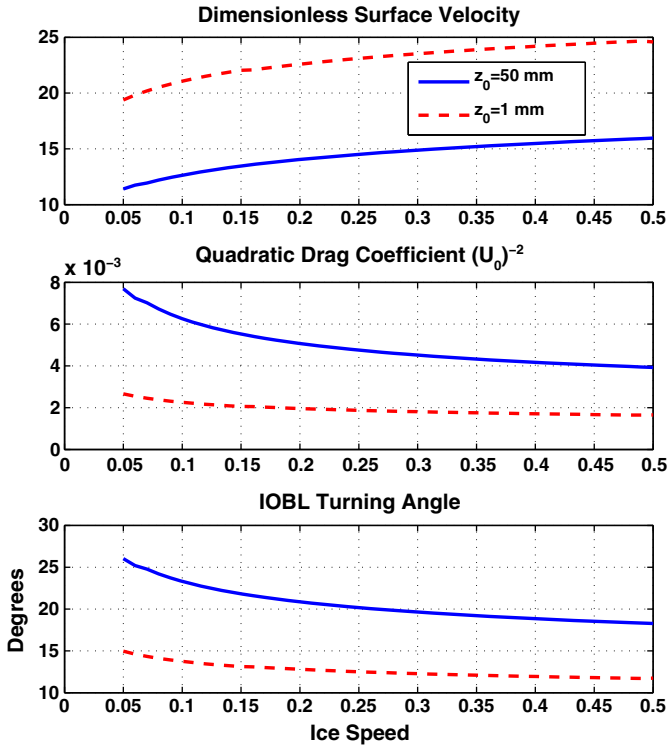

Fig. 5. Drag parameters as a function of ice speed, v_0, according to Rossby similarity, Eq. (13), for different values of z_0: 1 mm (thin, first year ice) and 50 mm (typical, multiyear pack ice).

How the Rossby similarity approach compares with the more traditional quadratic drag ($\hat{\tau}_0 = c_w v_0 \hat{v}_0 e^{\pm i\beta}$) is shown in Fig. 5 for wide but realistic ranges of ice speed and undersurface hydraulic roughness. In general, there is a marked decrease in the magnitude of the drag coefficient and the angle of turning with increasing velocity, especially for rougher ice. Similarly, smoother ice exerts much lesser drag on the ocean, and the turning angle is smaller, as illustrated by Fig. 4. From a least-squares analysis of the more general drag relation:

$$\tau_0 = a v_0^n \quad (15)$$

where a is an arbitrary constant, I found the exponent to be $n = 1.78 \pm 0.12$, using AIDJEX data taken from periods of free drift. In keeping with Rossby similarity, this was significantly different from quadratic (McPhee, 1979).

4. Impact of stratification

Stratification of the water column affects momentum transfer in two ways, both of which may become increasingly significant as a result of the changes now occurring in the Arctic. First, when ice is melting or freezing rapidly, buoyancy is introduced at the surface that reduces or enhances turbulence scales, with the effect of decreasing or increasing frictional coupling. Second, in polar oceans a layer of relatively cold and less saline water nearly always overlies saltier and often warmer water, separated from it by a sharp density gradient (pycnocline) in which turbulence is rapidly reduced. The depth and strength of the pycnocline are obviously of large interest in understanding changes in the distribution of heat and salt in the upper ocean, but generally are not thought to greatly influence drag, unless the pycnocline is shallow relative to the planetary scale.

4.1. Buoyancy flux at the ice–ocean interface

Buoyancy flux is defined in terms of the turbulent transport of density fluctuations in the upper ocean:

$$\langle w'b' \rangle = \frac{g}{\rho}\langle w'\rho' \rangle \quad (16)$$

where g is the acceleration of gravity, ρ' is deviation of density from its background state, ρ. For sea ice, the interface value of buoyancy flux, $\langle w'b' \rangle_0$, depends on the rate of melting or freezing.

A methodology termed *Monin–Obukhov similarity theory* is commonly utilized for treating the effect of buoyancy flux on turbulence in the atmospheric surface layer (e.g., Tennekes and Lumley, 1972). Obukhov (1971, English translation), demonstrated via dimensional analysis of the near surface wind (current) shear, that dimensionless shear in the surface layer, which by Eq. (9) is equal to unity for neutrally buoyant conditions, can be generalized to

$$\phi_m = \frac{\kappa|z|}{\hat{u}_{*0}}\frac{\partial \hat{u}}{\partial z} = \phi_m\left(\frac{\kappa|z|w'b'_0}{u_{*0}^3}\right) = \phi_m\left(\frac{|z|}{L_0}\right) \quad (17)$$

where $L_0 = u_{*0}^3/(\kappa\langle w'b' \rangle_0)$ is the Obukhov length. If L_0 is positive, turbulence must work against gravity, reducing the energy available for turbulent mixing, and *vice versa* for L_0 negative. If its magnitude is large (buoyancy flux small or stress large) relative to other scales, it has little impact on turbulence. Numerous studies in the atmospheric surface layer have resulted in fairly standard empirical functions for both stabilizing and destabilizing $\langle w'b' \rangle_0$ (e.g., Businger et al., 1971; Lettau, 1979).

Meltwater introduced at the ice/ocean interface stabilizes the boundary layer, and extracts energy from turbulence since work is required to mix the freshened water downward against the gravitational force. The impact is to decrease the governing

turbulence scale (λ_{max}), reducing the IOBL extent. Qualitatively, we anticipate that this has two effects on ice/ocean drag. First, for the same surface stress (u_{*0}), surface velocity magnitude will increase (drag decreases) because the frictional coupling between the ice and upper ocean is reduced. Second, the turning angle, β, will increase because z_0 (a physical as opposed to dynamic scale) is now larger relative to λ_{max}.

In McPhee (1981; see also 2008a, Section 4.3), I quantified these concepts in a similarity theory for the stably stratified IOBL that combined the planetary (u_{*0}/f) and Obukhov (L_0) scales in a stability factor, η_*, such that $\lambda_{max}=\eta_*^2\Lambda_* u_{*0}/f$ where:

$$\eta_* = \left(1+\frac{\Lambda_* u_{*0}}{\kappa R_c f L}\right)^{-1/2} = \left(1+\frac{\Lambda_* \mu_*}{\kappa R_c}\right)^{-1/2}.$$

The rationale behind the choice for η_* is that it forces λ_{max} to the following asymptotes:

$$\begin{array}{ll} \lambda_{max}\to\Lambda_* u_{*0}/f & \text{for} L_0\to\infty \\ \lambda_{max}\to R_c\kappa L_0 & \text{for } L_0\to 0^+ \end{array}$$

where R_c is the critical flux Richardson number (McPhee, 1981). The similarity hypothesis then requires that the length and velocity scales are modified to $\eta_* u_{*0}/f$ and $\hat{u}_{*0}/\eta_*$, respectively. For stabilizing buoyancy flux, $\eta_*\le 1$, thus melting reduces the turbulent length scale and increases the velocity scale.

By reasoning analogous to the neutral Rossby similarity derivation, it is straightforward (but algebraically involved) to formulate the dimensionless surface velocity ($\hat{U}_0=\eta_*\hat{v}_0/\hat{u}_{*0}$), and from that to generalize the inverse drag law to:

$$\hat{\Gamma}(Ro_*,\mu_*) = \frac{\hat{v}_0}{\hat{u}_{*0}} = \frac{1}{\kappa}[\log Ro_* - A(\mu_*) \mp iB(\mu_*)] \quad (18)$$

where $\mu_*=u_{*0}/(fL_0)$ is the ratio of the planetary to buoyancy (Obukhov) scales. Functional forms for the Rossby similarity parameters may be calculated from the theoretical dimensionless surface velocity (see Eq. 4.34 in McPhee, 2008a).

The impact of buoyancy flux from melting at the ice/ocean interface is demonstrated in Fig. 6, where ice velocity vectors for the same interfacial stress ($\hat{u}_{*0}=0.01$ m s^{-1}) and undersurface hydraulic roughness ($z_0=0.049$ m) are subject to different melting rates ranging from 0 to 30 cm/day. For the extreme melt rate (anticipated if the ice were drifting in 2 °C seawater), in one day the rapidly melting ice would drift about 6.4 km farther than ice with no melting.

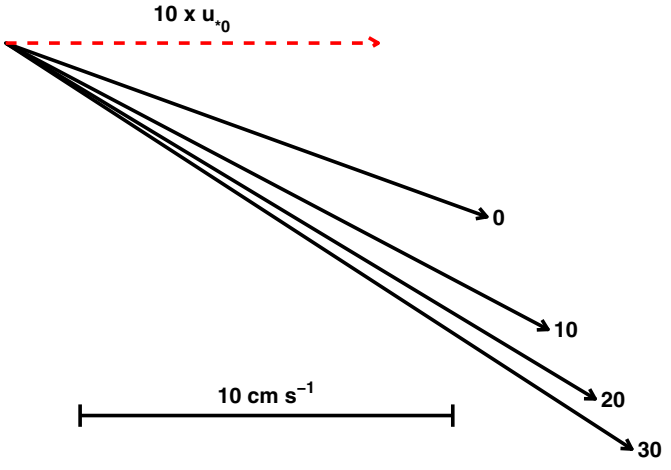

Fig. 6. Surface drift velocities for ice with the same interfacial stress and undersurface roughness, but different melt rates as indicated in cm per day by numbers with each vector.

Since intense melting of the leading edge of an ice pack drifting into warm water would cool the trailing water, we would expect a relatively narrow section of ice to drift away from the remaining pack. We suggested this (McPhee, 1983; Mellor et al., 1986) as a mechanism for forming separated ice bands often observed in marginal ice zones with off-ice winds (Martin et al., 1983).

When we first investigated the impact of rapid melt on ice dynamics, we thought the "slippery ice" phenomenon would be germane only in the marginal ice zones, when ice encountered water warm enough to provide buoyancy flux capable of substantially changing drag characteristics. Until recently summer mixed layer temperatures in the highly concentrated multiyear pack of the Arctic rarely reached temperatures more than a few tenths of a degree above freezing (e.g., Maykut and McPhee, 1995). Over the last several years, however, summer ice concentrations have often dropped to quite low values, and it is plausible that relatively large expanses of open water exist within the limits of the summer ice pack, with near surface temperatures reaching well above freezing. Consolidated ice drifting into these warm areas would tend to diverge because of the acceleration provided by melting, and in doing so, add to the positive ice-albedo feedback that seems to be such an important feature of the rapid decline in summer ice observed in recent years.

4.2. Impact of shallow pycnoclines

In the decades since the AIDJEX project, major changes in hydrography have accompanied changes in sea ice over the Canada Basin, exemplified by a comparison of average temperature and salinity profiles measured during the first 20 days of upper ocean data from AIDJEX station Caribou in May, 1975, and during a recent 20-day sample from Ice-Tethered Profiler #43 (http://www.whoi.edu/itp/; Krishfield and Perovich, 2005), beginning on 27 Dec 2010 (Fig. 7). During the twenty-day averaging intervals, each station passed within about 50 km of a particular geographic location: 75°N, 145°W, near the center of the (traditional) Beaufort Gyre. Both periods were also chosen to represent "late winter" conditions, past the period of rapid ice growth, and with the mixed layer near freezing. The obvious freshening at the ITP#43 site is consistent with results from a late winter International Polar Year hydrographic survey reported by McPhee et al. (2009). The ITP provides GPS position every half hour from which a velocity field was obtained after removing inertial components. During the 20-day period, buoy speeds ranged from almost zero to 0.37 m s^{-1}.

Assessing whether shoaling pycnoclines affect ice–ocean stress requires consideration of variation in eddy viscosity in the outer (Ekman) layer, which cannot be addressed with the simple similarity models described above. However, the similarity scaling may be incorporated into an algorithm for calculating a mixing length (λ) distribution through the well mixed layer and upper pycnocline (see Fig. 7.2 of McPhee, 2008a) that when multiplied by the *local* u_* provides an eddy viscosity distribution that varies through the entire IOBL. The method, *local turbulence closure* (LTC), may be incorporated into a time dependent numerical model that steps forward in time with prescribed external forcing, from specified initial conditions. It has been used to successfully simulate upper ocean observations made under various conditions (McPhee, 2008a, chapter 8).

Situations often arise (e.g., ship or aerial hydrographic surveys) for which there is not enough information to properly utilize a time-dependent numerical model (e.g., no time series of wind or advective fluxes). A variant on the LTC approach (McPhee, 1999) provides estimates of fluxes in the water column by assuming that turbulence adjusts instantaneously to changing surface conditions, and for which the T and S profiles, which determine density, are prescribed and held fixed. The SLTC (steady LTC) model utilizes an iterative process beginning from an initial estimate of surface stress and buoyancy flux, then successively refining estimates of buoyancy flux in the entire

IOBL by applying eddy diffusivity from the previous iteration to the prescribed T and S profiles. The new buoyancy flux determines eddy viscosity and stress for the next iteration, and the process is repeated until changes are small. The method is described in detail in McPhee (2008a, Ch. 9).

A thought experiment utilizing SLTC may be used to compare drag characteristics at Caribou and ITP#43 as follows. Consider a range of ice velocities from 0.05 to 0.4 m s^{-1}, with negligible melting or freezing ($\langle w'b'\rangle_0$). For each speed category, solve the SLTC model for u_{*0} twice, once for average T and S from AIDJEX, then again for the recent conditions as reported by ITP#43 (Fig. 7). In essence, the only difference in the two models is the depth of the pycnocline and the density gradient immediately below the well-mixed layer. The exercise demonstrates (Fig. 8) that across the range of speeds considered, variation in drag coefficient magnitude is relatively small, and that Rossby similarity, Eq. (13), (dashed curve) provides a good estimate of the model results. At higher speeds, however, the rightward deflection (β) in the shallow pycnocline model is about 10° larger than both the deep pycnocline model and the Rossby similarity formula. Model current hodographs for high (Fig. 9A) and moderate (Fig. 9B) surface stress illustrate why this variation in β occurs. IOBL volume transport (the integral of velocity perpendicular to surface stress) is perpendicular to interfacial stress, and proportional to its magnitude. At higher speeds, volume transport is confined to smaller vertical extent by the interaction between the pycnocline depth and the planetary scale (u_{*0}/f), resulting in larger transverse velocity through the entire well-mixed layer, including at the surface.

An aspect of strong stratification that is not addressed by the above exercise is drag generated by internal waves, which may be important when the well-mixed layer is quite shallow and interacts with an ice cover with significant pressure ridge keels and/or small floe sizes. We documented a period during the 1984 Marginal Ice Zone Experiment when internal wave (IW) drag appeared to be a major factor in the ice momentum balance (Morison et al., 1987), and developed a parameterization that could be incorporated into a relatively simple numerical model (McPhee and Kantha, 1989). We found that the impact of IW drag decreased rapidly with increasing mixed layer depth, and inferred that it would be of minor significance except in special circumstances, e.g., marginal ice zones when pack ice was in contact with warm water. As mentioned above, conditions in the western Arctic are often more highly stratified now than in the past, and there may be periods when IW drag is significant in ice/ocean exchange. For more details, the reader is referred to McPhee and Kantha (1989).

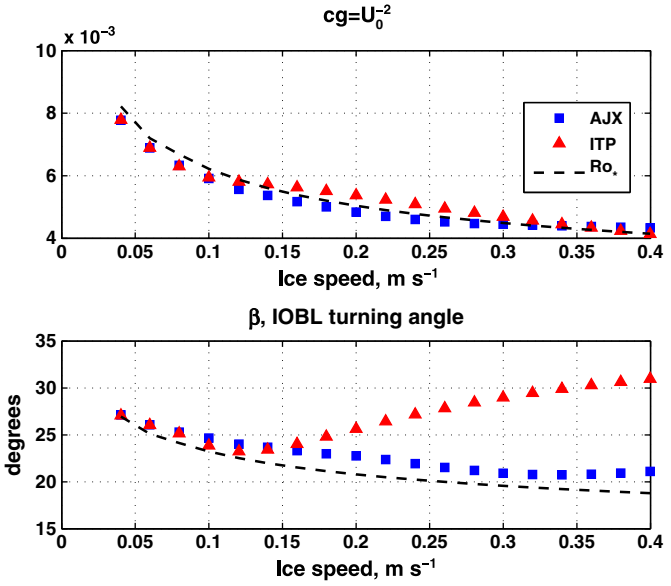

Fig. 8. Thought experiment examining the impact of shallow pycnocline in the recent (ITP) measurements on drag characteristics, as described in the text. Dashed lines indicate results from neutral Rossby similarity, Eq. (12).

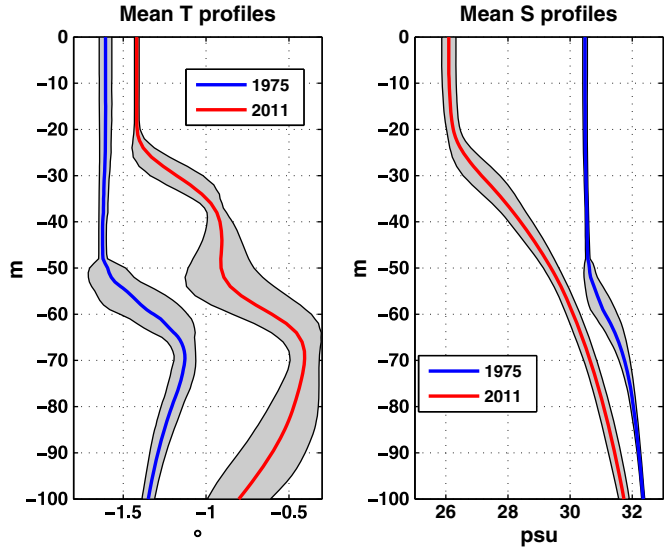

Fig. 7. Twenty-day average profiles from AIDJEX station Caribou in 1975 (blue) and Ice Tethered Profiler #43, 2011, when both were near a common location: 75°N and 145°W. Shaded envelopes indicate the standard deviations at each level.

An issue related to upper ocean stratification also not addressed by Rossby similarity is inertial oscillation, often manifested as cycloidal looping in ice drift trajectories. While observations, theory, and modeling of inertial oscillations are of obvious interest for many aspects of ice/ocean interaction (e.g., McPhee, 1978; Heil and Hibler, 2002; Kwok et al., 2003; Pritchard, this issue), it is important to note that measurements and modeling indicate that their impact on drag exerted by the IOBL on the ice undersurface is relatively minor (McPhee, 2008a, Section 8.2). For the most part the IOBL oscillates in phase with the ice, which means that measurements with instruments suspended from the drifting ice in the upper part of the IOBL will not detect inertial motion. Consequently, shear (thus stress) near the ice lacks much inertial component. A corollary is that in a situation with pronounced inertial motion, the "ice velocity relative to the undisturbed ocean" ($\hat{v}_0$) should be taken to exclude inertial components. A technique called complex demodulation for removing the inertial component from drift trajectories, is described by McPhee (1988).

5. Hydraulic roughness

Inspection of Figs. 4 and 5 indicates that the greatest variability in ice/ocean drag comes from variability of the underice surface roughness, z_0. I summarized (McPhee, 1990, Table 6.1) estimates from a number of different experiments and methods, and found wide variation, ranging from ~70 to 100 mm in old pack ice and in marginal ice zones, to hydraulically smooth under undeformed first-year ice.

During planning for the year-long, 1997–98 SHEBA project in the Canada Basin, we returned repeatedly to the issue of whether measurements made at one site were representative of the surrounding area up to the size of typical grid spacing in numerical models. This is particularly acute for the ice underside, because as a consequence of the

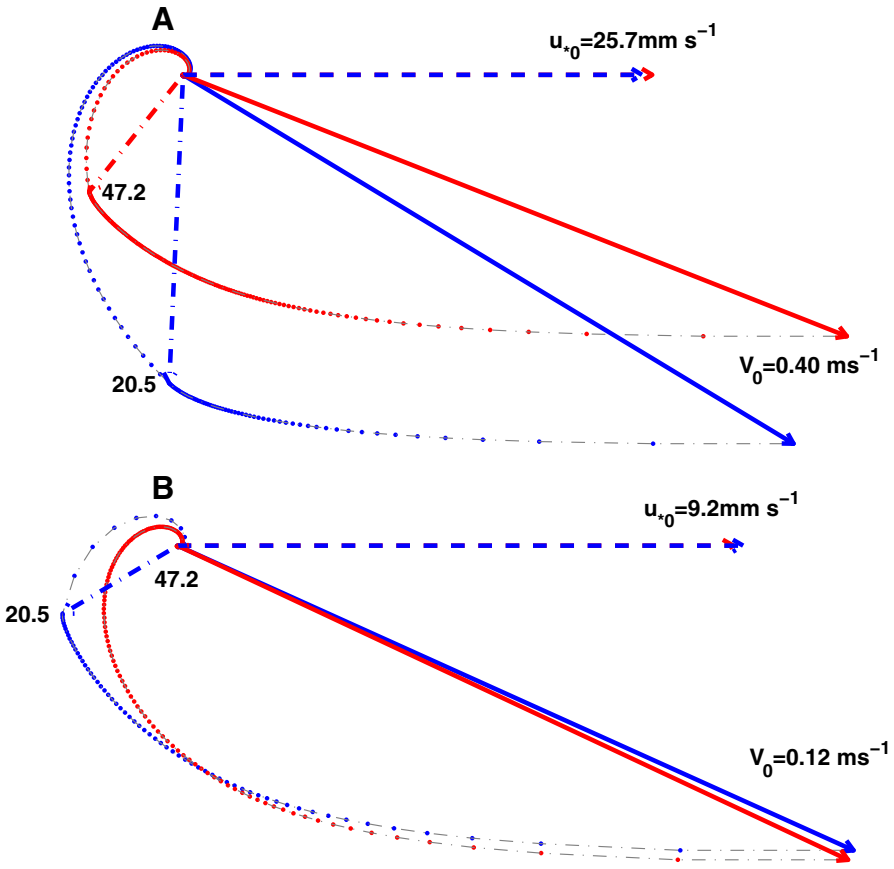

Fig. 9. Hodographs (plan views) of model IOBL currents for shallow (blue, ITP#43) and deep (red, AIDJEX Caribou) pycnoclines, and for both large surface stress (A) and typical surface stress (B). Numbers at the left indicate where the two pycnocline depths fall in the respective hodographs.

similarity scaling discussed in Section 3, physical scales in the atmospheric boundary layer are about 30 times (inverse square root of the density ratio) larger than in the IOBL. Consequently, whereas a 2-m pressure ridge sail represents only 1% or less of the typical atmospheric boundary layer extent, its isostatically compensated keel might occupy a third or more of the entire IOBL. Although large-eddy-simulation modeling of flow under two-dimensional ridge-like objects (e.g., Skyllingstad et al., 2003) can improve our understanding, determining how form drag from a fairly broad spectrum of ridge keels and floe boundaries affects overall drag is a difficult and mostly unsolved problem. There is also the practical aspect of siting instruments in ice that is smooth enough to work from, yet stable enough that the chances of its surviving ice deformation events is large. Our field measurements may thus systematically underestimate the actual stress and undersurface roughness representative of an entire large floe or region.

Measurements at multiple levels under sea ice often show that Reynolds stress increases with distance for several meters from the boundary, because at lower levels the stress includes turbulence generated by larger roughness elements farther away. An example (Fig. 10) from SHEBA illustrates this for two 6-h average profiles of friction speed measured at 4 levels under nearly identical current conditions: 0.2 m s^{-1} at 5 m (McPhee, 2002). In case A, the relative current was from a direction in which there was little apparent ice morphology. In case B, relative current approached from across a sizable pressure ridge about 110 m upstream. The solid curves are results from a horizontally homogeneous model with parameters chosen to match stress and velocity conditions at the uppermost cluster level, with estimated interfacial stress for case B nearly four times as large as case A, and a similar difference in drag coefficients.

The impact of upstream conditions on apparent roughness under a heterogeneous ice floe was even more dramatic during the ISPOL (Ice Station *Polarstern*) drift in the western Weddell Sea in 2004 (Hellmer

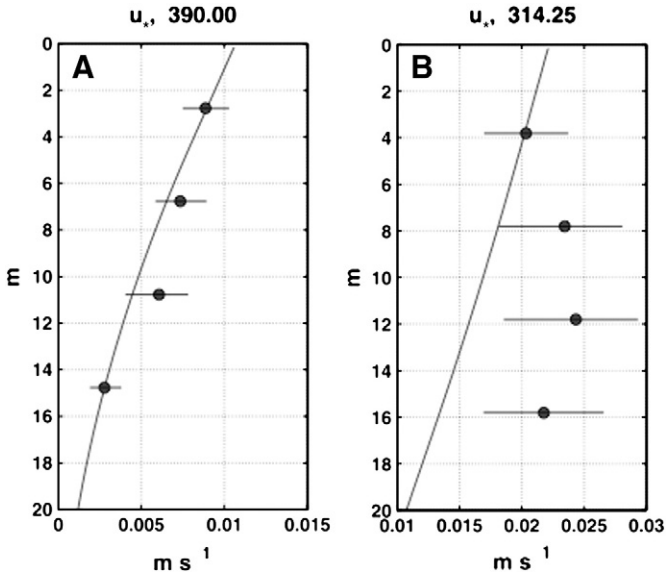

Fig. 10. Local friction speed (u_*) measurements during SHEBA when current speed at 5 m was nearly identical (0.2 m s^{-1}). A. 6-h average on centered on DOY 390.0 with no apparent upstream obstructions. B. 6-h average center at DOY 314.25, with large pressure ridge 110 m upstream.
Adapted from McPhee (2002).

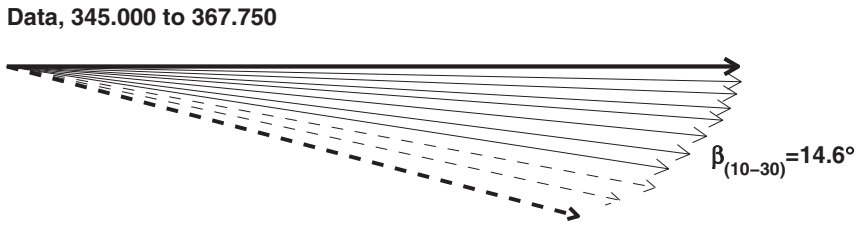

Fig. 11. Average non-dimensional current hodograph showing plan view of complex current ratios at each depth relative to 30 m, from 3-h ADP profiles. Solid arrows represent the entire ADP record of 82 3-h averages. Dashed arrows in the upper 3 bins are for ISPOL site 2 only, comprising 43 samples.
From McPhee (2008b).

et al., 2006). Based on differences in turbulence measurement level and location on the floe,[4] z_0 averaged from all directions still varied from 10 to 124 mm (McPhee, 2008). With the goal of characterizing its value for the entire ISPOL floe, I developed an indirect approach for estimating z_0. Over a wide range of current directions and magnitudes as measured by acoustic Doppler profiler, when I nondimensionalized current profiles by the complex velocity at 30 m, I found smoothly varying angular shear in the resulting average hodograph, with approximately 15° deviation between 10 and 30 m (Fig. 11). I reasoned that in the deeper part of the IOBL, the turbulence responsible for the observed angular shear would reflect conditions averaged over a large area, since the floe moved as a solid body. Using the SLTC model applied as described in McPhee (2008), I modeled each 3-h data segment, matching the measured current at 20 m, and using T and S profiles interpolated from the ship CTD data. For each 3-h model calculation, currents at the same level in the model as the measurements in Fig. 11, were nondimensionalized by the model current at 30 m. Then all of the model runs were averaged for comparison with the observations. This was done for three z_0 values ranging from 1 to 120 mm, as shown in Fig. 12. The middle value, 40 mm, coincided with the results of turbulence measurements 4 m below the ice at the first ISPOL site. Of the three values, it provides the most realistic angular shear in the lower IOBL (Fig. 12B). I then chose this value as representative of the entire ISPOL floe.

Since the method was first developed, it has been utilized to estimate floe (or area averaged) values for z_0 in other sites. Shaw et al. (2008) considered turbulence and profile data from unmanned buoys deployed near the North Pole. In one case, the buoy was deployed on an elongated floe, centered between two pressure ridges about 50 m apart. As might be expected, direction of relative flow had large impact on the turbulence and drag. When we applied the SLTC model as described above, we found that although flow direction mattered, directional variability in z_0 was reduced substantially. Overall we estimated floe-averaged z_0 to be about 90 mm.

A similar implementation of the SLTC model for the extensive SHEBA data set is described by McPhee (2008a, Section 9.3.2). In all I considered 249 separate 3-h model realization to arrive at a mean value for the logarithm of z_0 with standard deviation error bars of log $(z_0) = -3.0 \pm 1.0$. The mean value is about 49 mm, with a range implied by the standard deviation of log (z_0): 16 to 146 mm. The mean value agreed surprisingly well with the estimate for AIDJEX obtained from summer free-drift force balance (McPhee, 1980). It is interesting to compare this with a separate SHEBA study (McPhee, 2002) in which my objective was more or less the opposite: apply a combination of techniques to remove the impact of underice heterogeneity to arrive at z_0 values for *undeformed* multiyear sea ice. The result was about 6 mm, an order of magnitude smaller than the SLTC estimate.

[4] As in SHEBA, a breakup of the ISPOL floe necessitated moving the turbulence mast to a new location on the floe, with thinner ice and a nearby pressure ridge, where it remained for the last week of the project (McPhee et al., 2005).

Studies from fast ice in fjords or land locked channels (Langleben, 1982; Crawford et al., 1999; McPhee et al., 2008) have sometimes shown that the underside is *hydraulically smooth*, in which case the effective z_0 is a function only of stress and molecular viscosity. Hinze (1975) expression of the stress/velocity relationship over a smooth surface implies $z_{0s} \approx (\nu/u_{*0})e^2$ where ν is molecular viscosity. Typical values for z_{0s} are 3 to 5×10^{-5} m.

From turbulence measurements under thin (30–45 cm) first year ice in the Weddell Gyre during the MaudNESS project, Sirevaag et al. (2010) found that computing z_0 by standard (e.g., law-of-the-wall) techniques, implied values smaller than would be appropriate for a hydraulically smooth surface according to Hinze (1975). By applying the SLTC model, they showed that a more representative value was 4 mm, in line with earlier estimates from first year ice during the Antarctic Flux Experiment (ANZFLUX) in the Weddell: 2.2 mm and 1.3 mm for two drift stations, respectively (McPhee et al., 1999).

6. Discussion and recommendations

It seems to be common practice for modelers to express kinematic stress at the ice/water interface as a quadratic function of ice velocity following Eq. (1). The parameters are often treated as constant, with assigned values like $c_w = 0.0055$, $\beta = 23°$, derived from an analysis of AIDJEX drift in summer (Hibler, 1979; McPhee, 1980).

This paper is essentially a critical appraisal of that approach, based on extensive IOBL measurements, and also on the fact that the Arctic Ocean ice pack has changed dramatically since the time of AIDJEX. The critique falls into two areas, with the major points illustrated by Fig. 5. First, even if z_0 is known and relatively unchanging for a particular ice region, boundary layer physics dictates that effective drag magnitude will decrease with increasing speed, e.g., by about 1/3 over a range of expected speeds for $z_0 = 50$ mm, typical of multiyear pack ice. Similarly, for deep boundary layers (small stratification effect) β decreases by a few degrees (but not with shallow mixed layers, see Fig. 8). Second, undersurface roughness obviously plays a large role. Fig. 5 illustrates that for a given ice velocity, first year ice in the Weddell ($z_0 = 1$ mm) will exert half as much drag on the ocean, with β about half that of multiyear pack ice. This is borne out by drift speed to wind speed ratios: during summer at AIDJEX in 1975 (with "summer" indicated by the level of inertial oscillation) the ratio was 2.0% (McPhee, 1980) and slightly higher for SHEBA (~2.2%, for comparison see Fig. 11 of McPhee, 2002). By contrast, ratios for the two ANZFLUX drifts were 3.8% and 3.1%, respectively (McPhee et al., 1996). The deflection angle of ice drift from surface wind, which is a function of both the IOBL angle β and ice thickness, was around 47° for summer AIDJEX and about 16° for ANZFLUX.

While it may be apparent that z_0 affects drag magnitude, its impact on β is perhaps less appreciated. But consider the following thought experiment. Suppose that we are stationed on initially unstressed Arctic pack ice over a neutrally buoyant ocean, and are facing downwind near the boundary between large regions of rough ice ($z_0 = 50$ mm) to the left and smooth ice ($z_0 = 1$ mm) to the right, corresponding to the two conditions depicted in Fig. 5. (Since this is a

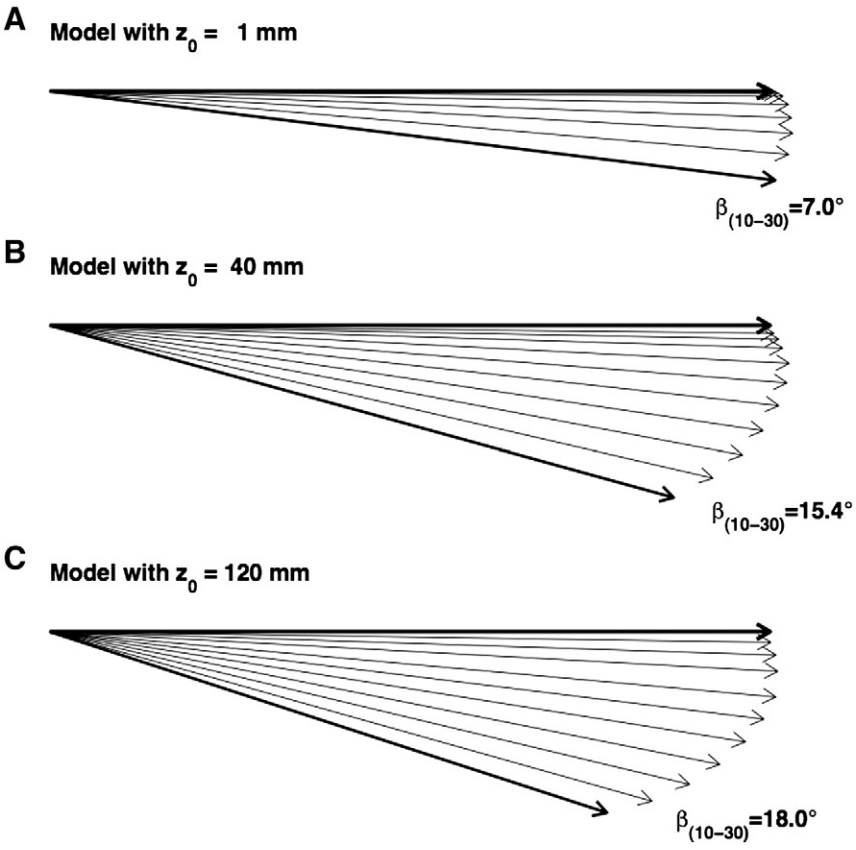

Fig. 12. Current hodographs from SLTC model applied to each 3-h sample, then nondimensionalized and averaged. Run B is closest to observed (Fig. 11). Adapted from McPhee (2008).

thought experiment, also imagine that ice Coriolis and wind stress forces are comparable.) As wind increases, the difference in drag coefficient magnitude (Fig. 5, middle) indicates that ice on the right will drift faster, and if we could ignore the difference in β, we would expect the two masses to drift with little interaction except in a narrow shear zone near where we stand. With these stipulations along with a steady wind providing a typical value of 10 mm s^{-1} for u_{*0}, over one day the ice on the right would drift about 20 km versus 12 km on the left. However, Fig. 5 (lower) suggests that β for ice on the left would be larger than that for the smoother region (about 20° versus 12°), hence there would be a tendency for the rougher ice to encroach on the thinner mass until the internal ice stress gradient across the boundary region was sufficient to counteract the rotational effects on the water stress. In other words, we would expect considerably more ice deformation (and we should probably move). With more first-year ice in the Arctic and decreasing overall thickness, it may become more important for models to account for these differences when considering ice dynamics.

Reported values for z_0 under sea ice range from hydraulically smooth ($\sim 10^{-5}$ m) to as much as 0.1 m, almost four orders of magnitude. It is justifiable to ask how this might be reasonably distilled to provide a useful but realistic parameterization of ice/ocean drag for numerical models. From my perspective the obstacles to this are twofold. First, both manned stations and unmanned data buoys (which are now capable of extremely useful boundary layer measurements [e.g. Shaw et al. 2008]) select the smoother parts of more substantial floes for deployment. There are two aspects to this; on the one hand, we run the risk of systematically underestimating drag by directly applying turbulence measurements; but on the other, by selecting thicker, multiyear floes we ignore the first-year, relatively thin ice that is now more and more prevalent in the Arctic.

A second obstacle has to do with the changing nature of the models themselves. For example, if an ice-ocean model carries enough vertical grid points to adequately resolve the IOBL, then in general one would apply a drag formulation to the difference in velocity ($\Delta\hat{u}$) between the ice and the uppermost grid point. If this falls within the surface layer (which changes dynamically), then usual surface layer techniques integrating the dimensionless shear equation would suffice. For neutral conditions,

$$\frac{\Delta\hat{u}}{\hat{u}_{*0}} = \frac{1}{\kappa}\log\frac{d_1}{z_0} \tag{19}$$

where d_1 is the separation between the ice and the first grid point. If rapid melting or freezing is present, then one might want to adjust this by standard Monin–Obukhov techniques. If the uppermost grid point falls within the outer layer, Eq. (19) would not be appropriate, and it might be better to approximate v_0 as the difference between ice velocity and the velocity at the uppermost grid point in the pycnocline, which would be close to the undisturbed, surface geostrophic flow.

With his own gentle style, Max Coon had a way of drawing succinct summaries out of (sometimes long winded) scientific discussions. So, it is not hard to imagine Max taking me to lunch (as he sometimes did when I was in Seattle or Bellevue) and after the usual banter and gossip about our polar colleagues, his getting serious and asking, “Well, Miles, after all these years, how are we to treat ocean drag in pack ice models?”

I would probably answer:

“First, Max, recognize that the drag relationship is not quadratic, particularly at higher drift speeds, and use something like Rossby

similarity Eq. (13) to estimate the magnitude of the geostrophic drag, Γ^{-1}. If the water is warm, you might want to include buoyancy effects as in Eq. (18), but make sure you keep track of the cooling left by ice melting."

"Second, if the pycnocline depth is large compared with the planetary scale, let β decrease with increasing ν_0 as in Eq. (13), but if not, maybe keep it about constant, say midrange for the particular z_0 in question. Unless the stratification persists almost to the ice/water interface, the magnitude of Γ from Eq. (13) is probably ok. There may be transient periods with high stratification when internal wave drag is a factor — in that case, lower Γ along the lines suggested by McPhee and Kantha (1989)."

"Third, regarding z_0: that's tricky, but here is how I would approach it. If the ice consists of identifiable, multiyear floes like the ones on all those projects we did back when, I would give it a value of about 40–60 mm. This describes pretty well AIDJEX, SHEBA, and even ISPOL in the western (multiyear) part of the Weddell. In the marginal ice zone, or with more highly deformed ice as in the buoy deployment described by Shaw et al. (2008), maybe doubling that would not be out of line. For thin, first year ice like we saw in the central Weddell, z_0 is much smaller: 2 mm is probably a decent choice. I suppose you want to know about a grid cell that contains a mixture. I think what I would do is use a weighted average of the logarithms of z_0 for the first and multiyear fractions. For special cases like undeformed fast ice, appreciate that drag may be very small, even with sizable tidal currents."

And finally…

"Ok, Max, enough science; let's find a place to sip a Scotch, and we'll talk over old times…"

Nomenclature

$\hat{v}_E$	Ekman velocity at the upper limit of the outer layer
c_w	quadratic water drag coefficient magnitude
β	angular shear across the IOBL, turning angle in the drag parameterization
$\hat{v}_0$	complex surface velocity relative to the "far field" (geostrophic) velocity
$\hat{\tau}_0$	complex kinematic boundary stress
$\hat{\tau}$	complex Reynolds stress: $\langle u'w'\rangle + i\langle v'w'\rangle$
$\hat{u}_{*0}$	complex boundary friction velocity:$\hat{\tau}_0 / \sqrt{\tau_0}$
f	Coriolis parameter
$\hat{u}$	velocity relative to far field
T	dimensionless turbulent stress: $\hat{\tau} / u_{*0}\hat{u}_{*0}$
U	dimensionless velocity (relative to far field)
ζ	dimensionless vertical coordinate
K_m	eddy viscosity
K_*	dimensionless eddy viscosity
δ	$\sqrt{i/K_*}$
u_τ	turbulent scale velocity
U_E	dimensionless Ekman velocity
c_{DE}	Ekman drag coefficient
ϕ_m	dimensionless current shear in the surface layer
κ	Kàrmàn's constant (0.4)
λ	mixing length
$K_{\max}$	maximum eddy viscosity
z_{sl}	surface layer extent
$\lambda_{\max}$	maximum mixing length
Λ_*	maximum dimensionless mixing length, similarity parameter ~0.028
$\Delta\hat{u}$	velocity difference across the surface layer
z_0	undersurface hydraulic roughness
A, B	Rossby similarity parameters
Γ	$\hat{v}_0 / \hat{u}_{*0}$, inverse geostrophic drag factor
Ro_*	surface friction Rossby number, $u_{*0}/(fz_0)$
$\langle w'b'\rangle$	buoyancy flux
$\langle w'b'\rangle_0$	interface buoyancy flux
L_0	Obukhov length scale $u_{*0}^3/(\kappa\langle w'b'\rangle_0)$
η_*	IOBL similarity stability parameter
R_c	critical flux Richardson number, ~0.2
μ_*	similarity stability parameter, $u_{*0}/(fL_0)$
u_*	local friction speed, $\sqrt{\tau}$
z_{0s}	hydraulic roughness for smooth surface
ν	molecular viscosity of sea water

Acknowledgments

The first acknowledgement is to Max Coon, a friend and mentor. Comments on the original manuscript by R. Pritchard and two anonymous reviewers were very helpful. Support for this work from the National Science Foundation under Grants 0906820; 0739371; and 0856214 is also gratefully acknowledged.

References

Blackadar, A.K., Tennekes, H., 1968. Asymptotic similarity in neutral planetary boundary layers. J. Atm. Sci. 25, 1015–1019.
Businger, J.A., Wyngaard, J.C., Izumi, Y., Bradley, E.F., 1971. Flux-profile relationships in the atmospheric surface layer. J. Atmos. Sci. 28, 181–189.
Crawford, G., Padman, L., McPhee, M., 1999. Turbulent mixing in Barrow Strait. Continental Shelf Res. 19, 205–245.
Deardorff, J.W., 1972. Numerical investigation of neutral and unstable planetary boundary layers. J. Atmos. Sci. 29, 91–115.
Ekman, V.W., 1905. On the influence of the earth's rotation on ocean currents. Ark. Mat. Astr. Fys. 2, 1–52.
Heil, P., Hibler III, W.D., 2002. Modeling the high-frequency component of Arctic sea ice drift and deformation. J. Phys. Oceanogr. 32 (11), 3039–3057.
Hellmer, H.H., Haas, C., Dieckmann, G.S., Schröder, M., 2006. Sea ice feedbacks observed in western Weddell Sea, EOS. Trans. Am. Geophys. Union 87 (18), 173–179.
Hibler III, W.D., 1979. A dynamic thermodynamic sea ice model. J. Phys. Oceanogr. 9, 815–846.
Hinze, J.O., 1975. Turbulence, Second ed. McGraw-Hill, New York. 790 pp.
Hunkins, K., 1966. Ekman drift currents in the Arctic Ocean. Deep-Sea Res. 13, 607–620.
Krishfield, R.A., Perovich, D.K., 2005. Spatial and temporal variability of oceanic heat flux to the Arctic ice pack. J. Geophys. Res. 110, C07021. doi:10.1029/2004JC002293.
Kwok, R., Cunningham, G.F., Hibler III, W.D., 2003. Sub-daily sea ice motion and deformation from RADARSAT observations. Geophys. Res. Lett. 30 (23). doi:10.1029/2003GL018723.
Langleben, M.P., 1982. Water drag coefficient of first-year sea ice. J. Geophys. Res. 87, 573–578.
Lettau, H.H., 1979. Wind and temperature profile prediction for diabatic surface layers including strong inversion cases. Boundary-Layer Meteorol. 17, 443–464.
Martin, S., Kauffman, P., Parkinson, C., 1983. The movement and decay of ice edge bands in the winter Bering Sea. J. Geophys. Res. 88, 2803–2812.
Maykut, G.A., McPhee, M.G., 1995. Solar heating of the Arctic mixed layer. J. Geophys. Res. 100, 24, 691–24, 703.
Maykut, G.A., Untersteiner, N., 1971. Some results from a time-dependent thermodynamic model of sea ice. J. Geophys. Res. 76, 1550–1575.
McPhee, M.G., 1978. A simulation of inertial oscillation in drifting pack ice. Dyn. Atmos. Oceans 2, 107–122.
McPhee, M.G., 1979. The effect of the oceanic boundary layer on the mean drift of sea ice: application of a simple model. J. Phys. Oceanogr. 9, 388–400.
McPhee, M.G., 1980. An analysis of pack ice drift in summer. In: Pritchard, R. (Ed.), Sea Ice Processes and Models. University of Washington Press, Seattle, pp. 62–75.
McPhee, M.G., 1981. An analytic similarity theory for the planetary boundary layer stabilized by surface buoyancy. Boundary-Layer Meterol. 21, 325–339.
McPhee, M.G., 1983. Turbulent heat and momentum transfer in the oceanic boundary layer under melting pack ice. J. Geophys. Res. 88, 2827–2835.
McPhee, M.G., 1988. Analysis and prediction of short term ice drift, transactions of the ASME. J. of Offshore Mech. and Arctic Engineer. 110, 94–100.
McPhee, M.G., 1990. Small scale processes. In: Smith, W. (Ed.), Polar Oceanography. Academic Press, pp. 287–334.
McPhee, M.G., 1994. On the turbulent mixing length in the oceanic boundary layer. J. Phys. Oceanogr. 24, 2014–2031.
McPhee, M.G., 1999. Scales of turbulence and parameterization of mixing in the ocean boundary layer. J Marine Systems 21, 55–65.

McPhee, M.G., 2002. Turbulent stress at the ice/ocean interface and bottom surface hydraulic roughness during the SHEBA drift. J. Geophys. Res. 107 (C10), 8037. doi:10.1029/2000JC000633.
McPhee, M.G., 2008a. Air–Ice–Ocean Interaction: Turbulent Ocean Boundary Layer Exchange Processes. Springer. ISBN 978-0-387-78334-5.
McPhee, M.G., 2008b. Physics of early summer ice/ocean exchanges in the western Weddell. Deep-Sea Res, II 55 (8/9), 1012–1022. doi:10.1016/j.dsr1012.2007.
McPhee, M.G., Kantha, L.H., 1989. Generation of internal waves by sea ice. J. Geophys. Res. 94, 3287–3302 1989.
McPhee, M.G., Martinson, D.G., 1994. Turbulent mixing under drifting pack ice in the Weddell Sea. Science 263, 218–221.
McPhee, M.G., Smith, J.D., 1976. Measurements of the turbulent boundary layer under pack ice. J. Phys. Oceanogr. 6, 696–711.
McPhee, M.G., Ackley, S.F., Guest, P., Huber, B.A., Martinson, D.G., Morison, J.H., Muench, R., Padman, L., Stanton, T.P., 1996. The Antarctic zone flux experiment. Bull. Am. Met. Soc. 77, 1221–1232.
McPhee, M.G., Kottmeier, C., Morison, J.H., 1999. Ocean heat flux in the central Weddell Sea in winter. J. Phys. Oceanogr. 29, 1166–1179.
McPhee, M.G., Kwok, R., Robins, R., Coon, M., 2005. Upwelling of Arctic pycnocline associated with shear motion of sea ice. Geophys. Res. Lett. 32, L10616. doi:10.1029/2004GL021819.
McPhee, M.G., Morison, J.H., Nilsen, F., 2008. Revisiting heat and salt exchange at the ice-ocean interface. Ocean flux and modeling considerations. J. Geophys. Res. 113, C06014. doi:10.1029/2007JC004383.
McPhee, M.G., Proshutinsky, A., Morison, J.H., Steele, M., Alkire, M.B., 2009. Rapid change in freshwater content of the Arctic Ocean. Geophys. Res. Lett. 36, L04606. doi:10.1029/2008GL036587.
Mellor, G.L., McPhee, M.G., Steele, M., 1986. Ice–seawater turbulent boundary layer interaction with melting or freezing. J. Phys. Oceanogr. 16, 1829–1846.
Morison, J.H., McPhee, M.G., Maykut, G.A., 1987. Boundary layer, upper ocean, and ice observations in the Greenland Sea marginal ice zone. J. Geophys. Res. 92, 6987–7011.
Nghiem, S.V., Rigor, I.G., Perovich, D.K., Clemente-Colon, P., Weatherly, J.W., Neumann, G., 2007. Rapid reduction of Arctic perennial sea ice. Geophys. Res. Lett. 34. doi:10.1029/2007GL031138.
Obukhov, A.M., 1971. Turbulence in an atmosphere with a non-uniform temperature. Boundary-Layer Meteorol. 2, 7–29.
Rossby, C.-G., 1932. A generalization of the theory of the mixing length with application to atmospheric and oceanic turbulence. Mass. Inst. Tech. Meteorol. Pap. 1 (4).
Shaw, W.J., Stanton, T.P., McPhee, M.G., Kikuchi, T., 2008. Estimates of surface roughness length in heterogeneous under-ice boundary layers. J. Geophys. Res. 113. doi:10.1029/2007JC004550.
Sirevaag, A., McPhee, M.G., Morison, J.H., Shaw, W.J., Stanton, T.P., 2010. Wintertime mixed layer measurements at Maud Rise, Weddell Sea. J. Geophys. Res. 115. doi:10.1029/2008JC005141.
Skyllingstad, E.D., Paulson, C.A., Pegau, W.S., McPhee, M.G., Stanton, T., 2003. Effects of keels on ice bottom turbulence exchange. J. Geophys. Res. 108 (C12), 3372. doi:10.1029/2002JC001488.
Smith, J.D., 1972. Surface boundary layer structure. AIDJEX Bulletin 14, 40–43.
Smith, J.D., 1974. Turbulent structure of the surface boundary layer in an ice-covered ocean. Rapp. P.-V. Reun., Cons. Int. Explor. Mer 167, 53–65.
Tennekes, H., Lumley, J.L., 1972. A First Course in Turbulence. MIT Press, Cambridge, MA. 300 pp.
Wyngaard, J.C., Cote, O.R., Rao, K.S., 1974. Modeling the atmospheric boundary layer. Advances in Geophysics 18A, 193–212 (Academic Press).